Density functional theory study on the copper(II) complex of benzimidazole

Rumyana Yankova[1], Lachezar Radev[2], Stoicho Avramov[3]

[1]Department of Inorganic and Analytical Chemistry, Asen Zlatarov University, 8010 Burgas, Bulgaria, r_iankova@yahoo.com

[2]Department of Fundamental Chemical Technology, University of Chemical Technology and Metallurgy, 1756 Sofia, Bulgaria, l_radev@abv.bg

[3]Navigation Faculty, Fac. № 131422, Nikola Vaptsarov Naval Academy, 9000 Varna, Bulgaria, stoicho3894@yahoo.com

Abstract—The geometry, electronic structure and chemical reactivity of a copper(II) complex of benzimidazole, are discussed on the basis of quantum chemical density functional theory calculations using B3LYP method with the 6-31G(d,p) basis set. The calculated highest occupied molecular orbital (HOMO) and lowest unoccupied molecular orbital (LUMO) with frontier orbital gap were presented. Frontier molecular orbital analysis showed that the energies of HOMO and LUMO orbitals are –5.8875 and –0.9546 eV, respectively. The experimental infrared spectrum was compared with calculated and complete vibrational assignment was provided. The electrostatic potential was calculated in order to investigate the reaction properties of the molecule.

Keywords— copper(II) complex of benzimidazole, quantum chemical calculations, geometry optimization, electronic properties

I. INTRODUCTION

The heterocycles are one of the largest areas of research in organic chemistry for more than a century. They are good ligands due to the presence of possible coordination sites. Their biological activities and unique structures are reason for this interest. They have applications in different areas of pharmaceutical and agrochemical research or, more recently, in material sciences [1]. Benzimidazole is extensively used in industrial processes as a corrosion inhibitor for metal and alloy surfaces [2-5]. It is also known to play a fundamental role in many biological systems [6,7]. Metal complexes of biologically important ligands are more effective than free ones [8].

To design more effective metal complexes with benzimidazole, predict their properties and choose a more suitable one for a specific application, theoretical study at the molecular level seems to be necessary. A great number of advanced molecular theories related to study of geometry, electronic states and chemical reactivity of the chemical compounds are reported [9-13]. The use of density functional theory (DFT) makes an important contribution to promotion of theoretical calculations. In this work, a theoretical study on the geometry, electronic structure and chemical reactivity of the dibromobis(benzimidazole)Cu(II) complex by density functional theory (DFT) calculations using B3LYP method with the 6-31G(d,p) basis set was carried out.

II. EXPERIMENTAL AND COMPUTATIONAL SECTION

1. Synthesis of dibromobis(benzimidazole) Cu(II) complex

The [Cu(benzimidazole)$_2$Br$_2$] complex was prepared according to the method outlined by M. Bukowska-Strzyzewska and A. Tosik [14]. The infra-red spectra were recorded on a Bruker Tensor 27 FT-IR spectrometer in the 4000 – 400 cm^{-1} range, with the samples embedded in KBr matrixes. The thermos-gravimetric analysis was performed on an apparatus STA 449 F3 JUPITER (Netzsch) for TG-DTG/DSC at heating rate 10°C min^{-1} from room temperature to 1000°C under flowing air (20 cm^3 min^{-1}).

2. Calculation details

Calculations were performed using DFT method subjected to the gradient-corrected hybrid density functional B3LYP method. This function is a combination of the Becke's three parameters potential with the hybrid correlation functional of Lee-Yang-Parr (B3LYP) [15-17]. The geometry optimization was performed using the 6-31G(d,p) basis set. Results were visualized using GaussView 5 software package [18]. All calculations were converged to 10^{-8} a.u. The optimized structural parameters were used in the vibrational frequency calculations at the DFT level to characterize the stationary point as minima. The frontier molecular orbital (FMO) theory was used [19]. All calculations were performed in Gaussian 03 program package [20].

III. RESULTS AND DISCUSSION

1. Geometry optimization

The optimized geometrical parameters (bond lengths, valence angles and selected dihedral angles) were computed by B3LYP method with 6-31G(d,p) and are summarized in Table 1. For comparison, experimental X-ray crystal data obtained by M. Bukowska-Strzyzewska and A. Tosik [14] are also

presented. The optimised molecular geometry of the complex with atom numbering is shown in Figure 1.
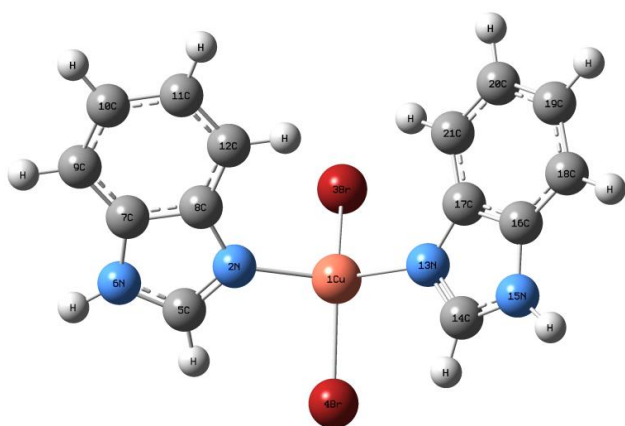

Figure 1. Optimized crystal structures and atom numbering of dibromobis(benzimidazole)Cu(II) complex

Table 1. Experimentaly determined structural parameters of dibromobis(benzimidazole)Cu(II) complex [14] and theoretically calculated using B3LYP/6-31G(d,p)

Structural parameters	B3LYP 6-31G(d,p)	X-ray data
Bond length (Å)		
$Cu^1–N^2$	1.991	1.976
$Cu^1–N^{13}$	2.022	1.946
$Cu^1–Br^3$	2.334	2.446
$Cu^1–Br^4$	2.369	2.402
$N^2–C^5$	1.316	1.32
$N^{13}–C^{14}$	1.320	1.33
$C^5–N^6$	1.359	1.35
$C^{14}–N^{15}$	1.356	1.35
$N^6–C^7$	1.389	1.36
$N^{15}–C^{16}$	1.388	1.37
$C^7–C^8$	1.409	1.40
$C^{16}–C^{17}$	1.411	1.40
$C^8–N^2$	1.392	1.38
$C^{17}–N^{13}$	1.400	1.40
$C^7–C^9$	1.395	1.39
$C^{16}–C^{18}$	1.396	1.40
$C^9–C^{10}$	1.391	1.36
$C^{18}–C^{19}$	1.390	1.37
$C^{10}–C^{11}$	1.410	1.41
$C^{19}–C^{20}$	1.409	1.40
$C^{11}–C^{12}$	1.389	1.37
$C^{20}–C^{21}$	1.390	1.39
$C^{12}–C^8$	1.398	1.39
$C^{21}–C^{17}$	1.400	1.38
Valence angle (degree)		
$Br^4–Cu^1–N^2$	95.2	95.0
$Br^4–Cu^1–N^{13}$	97.8	94.8
$Br^3–Cu^1–N^2$	94.9	93.7
$Br^3–Cu^1–N^{13}$	101.6	94.1
$Br^3–Cu^1–Br^4$	138.6	139.0
$N^2–Cu^1–N^{13}$	136.6	105.8
$Cu^1–N^2–C^8$	127.9	128.0
$Cu^1–N^{13}–C^{17}$	131.5	127.9
$Cu^1–N^2–C^5$	125.1	125.0
$Cu^1–N^{13}–C^{14}$	122.1	126.0
$N^2–C^5–N^6$	111.9	111.6
$N^{13}–C^{14}–N^{15}$	112.3	112.3
$C^5–N^6–C^7$	107.9	108.8
$C^{14}–N^{15}–C^{16}$	107.9	107.4
$N^6–C^7–C^8$	104.8	104.7
$N^{15}–C^{16}–C^{17}$	105.0	106.7
$C^7–C^8–N^2$	108.9	109.5
$C^{16}–C^{17}–N^{13}$	108.8	107.8
$C^8–N^2–C^5$	106.3	105.5
$C^{17}–N^{13}–C^{14}$	105.9	105.8
$C^7–C^9–C^{10}$	116.5	117.6
$C^{16}–C^{18}–C^{19}$	116.5	116.2
$C^9–C^{10}–C^{11}$	121.6	121.2
$C^{18}–C^{19}–C^{20}$	121.3	121.8
$C^{10}–C^{11}–C^{12}$	121.6	121.3
$C^{19}–C^{20}–C^{21}$	121.8	121.6
$C^{11}–C^{12}–C^8$	117.4	118.5
$C^{20}–C^{21}–C^{17}$	117.5	117.4
$C^{12}–C^8–C^7$	120.5	119.5
$C^{21}–C^{17}–C^{16}$	119.9	120.6
$C^8–C^7–C^9$	122.3	121.9
$C^{17}–C^{16}–C^{18}$	122.7	122.4
$N^6–C^7–C^9$	132.8	133.4
$N^{15}–C^{16}–C^{18}$	132.2	130.9
$N^2–C^8–C^{12}$	130.5	130.9
$N^{13}–C^{17}–C^{21}$	131.3	131.6
Dihedral angle (degree)		
$C^8–N^2–N^{13}–C^{17}$	– 16.5	–
$C^8–N^2–Cu^1–Br^3$	– 62.3	–
$C^{17}–N^{13}–Cu^1–Br^3$	37.6	–
$C^8–N^2–Cu^1–Br^4$	157.8	–
$C^{17}–N^{13}–Cu^1–Br^4$	–178.9	–
$C^5–N^2–Cu^1–Br^4$	–32.0	–
$C^{14}–N^{13}–Cu^1–Br^4$	–6.9	–

In general, the calculated structural parameters match well with experimental data with few exceptions. The difference found in calculated values (in gas phase) from the experimental values may be due to solid state intermolecular interactions related to crystal packing effects. Based on above comparison, although there are some differences between the theoretical and the experimental values, the optimized structural parameters can well reproduce the experimental ones and they are the bases for thereafter discussion.

2. Frontier molecular orbital (FMO) analysis

The frontier molecular orbitals are very important parameters for quantum chemistry since they are used for investigation of stability and reactivity of molecules [21]. A smaller energy difference ($E_{LUMO} − E_{HOMO}$) between the lowest unoccupied molecular orbital (LUMO) and the highest occupied molecular orbital (HOMO) would determine a larger reactivity. In addition, the HOMO primarily acts as an electron donor and the LUMO largely acts as the electron acceptor. The energies of HOMO, LUMO and their orbital energy gap are calculated using B3LYP/6-31G(d,p) (Table 2). Illustration of the frontier molecular orbitals and their respective positive and negative regions obtained by DFT method for dibromobis(benzimidazole)Cu(II) complex are shown in Figure 2. Results showed that HOMO is delocalized on the bromine atoms as the contribution (ψ_{HOMO}) involves their *p*-orbitals: 18.8% $9p_y(Br^3)$ + 14.6% $10p_y(Br^3)$ + 7.9% $9p_z(Br^3)$ + 6.8% $10p_z(Br^3)$ − 5.8% $8p_y(Br^3)$ + 4.4% $9p_y(Br^4)$. Unlike HOMO, LUMO is delocalized on the one benzimidazole ligand and the

(ψ_{LUMO}) includes mainly the *p*-orbitals of the carbon atoms: 13.7% $3p_z(C^5)$ + 11.7% $2p_z(C^5)$ + 10.7% $3p_z(C^9)$ + 10.4% $3p_z(C^{12})$ + 7.7% $2p_z(C^{12})$ + 7.0% $2p_z(C^9)$.
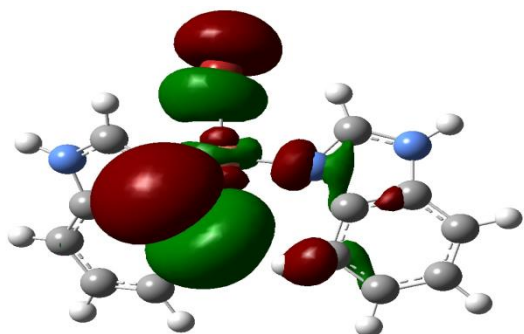
1
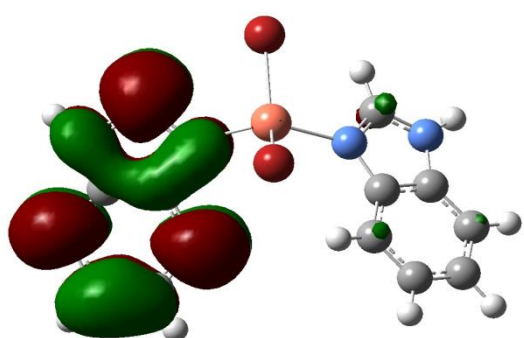
2

*Figure 2. Electron distribution of HOMO – **1** and LUMO – **2** for dibromobis(benzimidazole)Cu(II) complex*

2.1. HOMO–LUMO theory

TThe HOMO and LUMO energy values are related to the ionization potential (*I*) and electron affinities (*A*) [22]:

$$I = -E_{\text{HOMO}}$$

$$A = -E_{\text{LUMO}}$$

The difference between HOMO and LUMO energy values gives the energy gap (E_{LUMO}–E_{HOMO}). Using HOMO and LUMO energy values and approximations of Koopman's theorem [23], the global quantum molecular descriptors such as global (chemical) hardness (*η*) and softness (*σ*), electronegativity (*χ*), chemical potential (*µ*) and electrophilicity index (*ω*) were calculated (Table 2). The sections below describe the theoretical backgrounds of above mentioned properties.

2.2. Global hardness and softness

In the simplest terms, the hardness of a species (atom, ion, or molecule) is a qualitative indication of how polarizable it is. In other words, the hardness of a species indicates how much its electron cloud is distorted in an electric field. The hardness and softness were suggested in literature [24] to denote resistance to deformation by mechanical force. This explains the changes in the energy linked with the transition state to ground-state using different descriptors. The softness is simply the reciprocal of the hardness. The global hardness (*η*) and softness (*σ*) of a chosen molecule calculates the energy gap between the HOMO and LUMO orbitals. The mathematical expression of (*η*) and (*σ*) can be written as:

$$\eta = \frac{I - A}{2} = \frac{E_{\text{LUMO}} - E_{\text{HOMO}}}{2}$$

$$\sigma = \frac{1}{2\eta} = \frac{1}{I - A} = \frac{1}{E_{\text{LUMO}} - E_{\text{HOMO}}}$$

Molecules with large HOMO–LUMO energy gap are hard which implies higher stability and opposing charge transfer, since they oppose changes in their electron density and distribution. On the contrary, molecules which require a small $E_{\text{LUMO–HOMO}}$ for its excitation are termed as soft molecules. Hence, they are highly polarizable in nature. In terms of chemical change, soft molecules are more reactive than hard molecules.

2.3. Electronegativity

Electronegativity is the tendency of molecules to attract electrons [25]. Parr and Yang attempted to quantify this descriptor [26]. This is found by the average of HOMO and LUMO energy values. It can be expressed in terms of orbital energies:

$$\chi = -\frac{E_{\text{HOMO}} - E_{\text{LUMO}}}{2} = \frac{I + A}{2}$$

In the light of this, the electronegativity of a molecule is the drop in energy when an infinitesimal amount of electronic charge is added to the system. It is a measure of resistance of an atom or ion, or a group or atoms in a molecule for an entering electronic charge.

2.4. Chemical potential

Chemical potential denotes the affinity of an electron to escape and is defined as the first derivative of the total energy with respect to the number of electrons in a molecule [27]. By the expression of MO theory, *µ* is simply the negative of electronegativity value. It is given as:

$$\mu = -\chi = \frac{E_{\text{HOMO}} + E_{\text{LUMO}}}{2} = -\frac{I + A}{2}$$

2.5. Electrophilicity index

The capability of a substance to accept electrons is quantified as electrophilicity index (ω). Parr et al. [28] defined the electron affinity as the capability of a substance to have only one electron from the surroundings. This index measures the energy lowering of a substance due to the electron flow between donor and acceptor. Parr and co-workers suggested that ω can be measured through the equation:

$$\omega = \frac{\mu^2}{2\eta} = \frac{\left[\left(\frac{E_{HOMO} - E_{LUMO}}{2}\right)^2\right]}{E_{LUMO} - E_{HOMO}} = \frac{\left[\left(\frac{I + A}{2}\right)^2\right]}{I - A}$$

Table 2. Calculated E_{HOMO}, E_{LUMO}, energy band gap ($E_{LUMO-HOMO}$) and quantum molecular descriptors at 298.15 K for dibromobis(benzimidazole)Cu(II) complex

E_{HOMO}	E_{LUMO}	$E_{LUMO-HOMO}$	χ	μ	η	σ	ω
(eV)	(eV)	(eV)	(eV)	(eV)	(eV)	(eV)	(eV)
−5.88	−0.95	4.93	3.42	−3.42	2.47	0.20	2.37

3. Molecular electrostatic potential (MEP)

The distribution of electrical charge (electrons and nuclei of a molecule) creates an electrostatic potential ($V(r)$) in the surrounding space [29]. The electrostatic potential is a real physical property, very useful for analyzing and predicting molecular reactive behavior. It is strictly defined and can be determined experimentally as well as computationally. The electrostatic potential has been particularly useful as an indicator of the sites or regions of a molecule to which an approaching electrophile or nucleophile is initially attracted, and it has also been applied successfully to the study of interactions that involve a certain optimum relative orientation of the reactants [30]. The positive point charge is attracted to those regions in which $V(r)$ is negative, since this leads to negative (stabilizing) interaction energy. In addition, the positive point charge is repelled from regions of positive potential, in which the interaction energy is positive and destabilizing.

If a molecule has an electronic density function $p(r)$, then its electrostatic potential at any point r' can be calculated by the expression:

$$V_{(r)} = \sum_A \frac{Z_A}{|R_A - r|} - \int \frac{\rho(r')}{|r' - r|} dr$$

where, Z_A is the charge on the nucleus A, located at distance R_A. The first term on the right side of the expression denotes the contribution of the nuclei, which is positive. The second term brings in the effect of the electrons, which is negative. The presented expression is an exact formula for the electrostatic potential due to the set of nuclei (Z_A) and the electronic density function $p(r)$. On the other hand, the latter function is generally obtained from molecular wave function and is accordingly approximate. Therefore, the resulting electrostatic potential showed be possesses an approximate character.

The total electron density and molecular electrostatic potential surface of the dibromobis(benz-imidazole)Cu(II) complex are calculated using B3LYP/6-31G(d,p) method. The total electron density mapped with electrostatic potential surface is shown in Figure 3. Different colors were denoted for various values of the electrostatic potential. Deepest red colour corresponds to the electron rich regions, localized most negative charge (–0.05862 a.u.). In contrary, dark blue colour symbolizes the electron deficient areas, i.e. is corresponds to the most positive charge (+0.06652 a.u.). Therefore, dark blue colour characterizes the nucleophilic reactivity of the dibromobis(benzimi-dazole)Cu(II) complex.
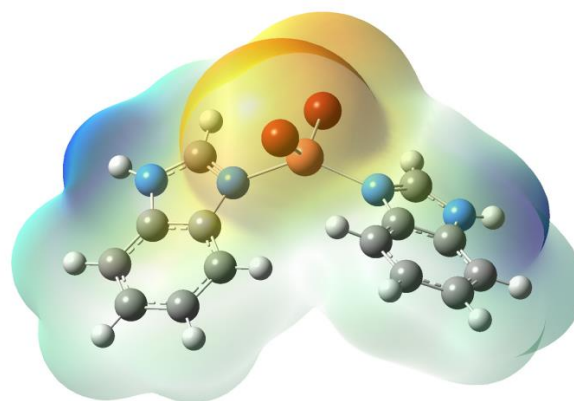

Figure 3. Molecular electrostatic potential surface for the dibromobis(benzimidazole)Cu(II) complex

The electrostatic potential contour map for positive and negative potentials is shown in Figure 4. It is obviously that the region around bromine atoms represents the most negative potential region (deepest red). In contrary, the maximum amount of positive charge (dark blue) was registered on the nitrogen atoms N^6 and N^{15}.
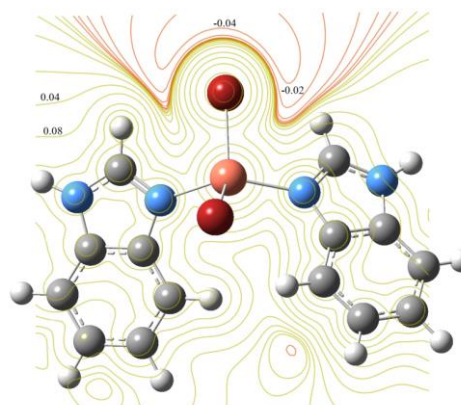

Figure 4. Molecular electrostatic potential contour for dibromobis(benzimidazole)Cu(II) complex

4. *Vibrational Spectral Analysis*

The harmonic vibrational frequencies for dibromobis(benzimidazole)Cu(II) complex were calculated by using the DFT method with B3LYP functional and 6-31G(d,p) basis set. The observed vibrational spectra are given in Figure 5. The corresponding frequencies along with the assignments and intensities are given in Table 3. Comparison between the calculated and the observed vibrational spectra helps us to understand the observed spectral features. It can be seen that the experiment has a good coincidence with the calculations (after scaling [31]). The calculations were done on a single molecule in the gaseous state while the experimental values recorded in the presence of intermolecular interactions. Therefore are noted any discrepancy between the observed and the calculated frequencies.
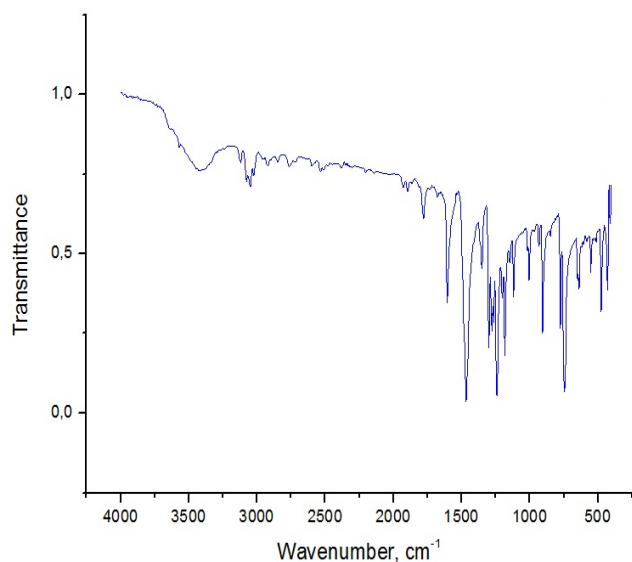

Figure 5. Experimental IR spectrum of dibromobis(benzimidazole)Cu(II) complex

The theoretically computed values of the C–H stretching vibrations (3284 – 3212 cm^{-1}) are in good agreement with the data from literature [32,33]. The frequencies 1284, 1180, 1152, 1133 and 995 cm^{-1} are assigned to C–H in-plane bending vibrations and coincides well with literature data [34,35]. Hence the bands at 767, 640 and 556 cm^{-1} are assigned to give C–H out-of-plane bending vibration. Tsuboi [36] reported the N–H stretching frequency at 3481 cm^{-1} in aniline. In the present work (N–H) stretching is assigned to the band at 3675 cm^{-1}. The N–H in-plane bending and N–H out-of-plane bending are assigned to the bands at 1448 and 516 cm^{-1} which agrees well with Venkateswaran and Pandya [37] and Evans [38]. Pinchas et al. [39] assigned the C–N stretching band at 1368 cm^{-1} in benzamide. Kahovec and Kohlreusch [40] identified the stretching frequency of the C=N band in salicylic aldoxime at 1617 cm^{-1}. Refering to the above workers, the bands at 1300 cm^{-1} and 1501 cm^{-1} are assigned to C–N and C=N stretching, respectively.

The vibrational frequencies at 1679 and 1677 cm^{-1} are assigned to C=C stretching. The vibrational frequencies at 307, 291 and 248 cm^{-1} are theoretically assigned to Cu–Br and Cu–N stretching, respectively.

Table 3. Some experimental and calculated characteristic frequencies (cm^{-1}), IR intensity and probable assignments of dibromobis(benzimidazole)Cu(II) complex

Calculated frequencies	I_{Abs}	Experimental frequencies	Assignments
3677; 3675	100	3430 *w*	$v_{(N-H)}$ *ipb*
3284	22	3125 *w*	$v_{(C-H)}$ *ipb*
3268; 3212	49	3081 *w*	$v_{(C-H)}$ *ipb*
1679	7	1605 *s*	$v_{(C=C)}$, *Rband*
1677	7	1586 *w*	$v_{(C=C)}$, *Rband*
1556; 1546	73	1480 *w*	$v_{(C=N)}$, *Rband*
1501	23	1500 *w*	$v_{(C=N)}$, *Rband*
1448	64	1467 *s*	$v_{(N-H)}$ *ipb, Rband*
1349	10	1351 *s*	*Rband*
1304; 1300	31	1300 *s*	$v_{(C-N)}$, *Rband*
1284	48	1277 *s*	$v_{(C-H)}$ *ipb, Rband*
1216	7	1265 *m*	*Rband*
1213	20	1241 *s*	*Rband ipb*
1181	2	1201 *s*	*Rband ipb*
1180	2	1183 *m*	$v_{(C-H)}$ *ipb*
1152	16	1148 *s*	$v_{(C-H)}$ *ipb*
1133	35	1118 *s*	$v_{(C-H)}$ *ipb*
995	1	1005 *w*	$v_{(C-H)}$ *ipb*
979	12	932 *s*	*Rband ipb*
897	7	906 *m*	$v_{(C-H)}$ *ipb, Rband*
775	4	775 *s*	$v_{(C-H)}$ *opb*
762	81	747 *m*	$v_{(C-H)}$ *opb, Rband*
640	1	640 *s*	$v_{(C-H)}$ *opb, Rband*
556	2	553 *w*	$v_{(C-H)}$ *opb, Rband*
516	96	476 *s*	$v_{(N-H)}$, *opb Rband*
444; 434	19	430 *s*	*Rband opb*
307; 291	17	–	$v_{(Cu-Br)}$
248	28	–	$v_{(Cu-N)}$

Scale factors of 0.9613 for calculated frequencies with B3LYP/6-31G(d,p)
s - strong; *m* - medium; *w* - weak; *vw* - very weak
v - stretching; *Rband* – ring deformation; ipb – in-plane bending; opb – out-of-plane bending
I_{Abs}-Theoretical infrared intensities

IV. CONCLUSION

Dibromobis(benzimidazole)Cu(II) complex was synthesized. The complete molecular structural parameters, electronic structure and chemical reactivity were calculated with DFT-B3LYP methods using 6-31G(d,p) basis set. Quantum chemical descriptors such as global hardness and softness, chemical potential, electronegativity and electrophilicity index, HOMO–LUMO energy gap and HOMO/LUMO energy were studied. Molecular electrostatic potential analysis showed that the most negative charge is localized around bromine atoms, while a large electropositive potential is observed in the area of the benzimidazole ligands. The vibrational frequencies of the fundamental modes of the compound were precisely assigned, analyzed and the theoretical results were compared with the experimental vibrations.

REFERENCES

[1] García-Valverde M., T. Torroba, Sulfur-nitrogen heterocycles, (2005) 318–320.

[2] Materazzi, S., R. Curini, G. D'Ascenzo, Thermoanalytical study of benzimidazole complexes with transition metal ions: Copper (II) complexes, Thermochimica acta, 286 (1996) 1–15.

[3] Faltermeier, R.B., A corrosion inhibitor test for copper-based artifacts, Studies in Conservation, 44 (1999) 121–128.

[4] Khaled, K.F., The inhibition of benzimidazole derivatives on corrosion of iron in 1 M HCl solutions, Electrochimica Acta, 48 (2003) 2493–2503.

[5] Obot, I.B., N.O. Obi-Egbedi, Theoretical study of benzimidazole and its derivatives and their potential activity as corrosion inhibitors, Corrosion Science, 52 (2010) 657–660.

[6] A.A. Spasov, I.N. Yozhitsa, L.I. Bugaeva, V.A. Anisimova, Benzimidazole derivatives: Spectrum of pharmacological activity and toxicological properties, Pharmaceutical chemistry Journal, 33 (1999) 232–243.

[7] S.O. Podunavac-Kuzmanovic, V.M. Leovac, N.U. Perisic-Janjic, J. Rogan, J. Balaz, Complexes cobalt (II), zinc (II) and copper (II) with some newly synthesized benzimidazole derivatives and their antibacterial activity, Journal of the Serbian Chemical Society, 64 (1999) 381–388.

[8] I.S. Ahuja, I. Prasad, Isonicotina¬mide complexes with some metal (II) halides and pseudohalides, Inorganic and Nuclear Chemistry Letters, 12 (1976) 777–784.

[9] Yankova, R., L. Radev, Structural and Electronic Properties of [Co(benzimidazole)2I2], International Journal of Materials and Chemistry, 6 (2016) 19–27.

[10] Yankova, R., Natural Bond Population Analysis of dichlorobis(benzimidazole)Co(II) complex, Physical Chemistry: An Indian Journal, 11 (2016) 1–6.

[11] Yankova, R., Study on dibromobis(benzimida-zole)Co(II) complex. I. Molecular structure and vibrational analysis, Industrial Thechnologies, 3 (2016) 146–150.

[12] Yankova, R., Study on dibromobis(benzimida-zole)Co(II) complex. II. Natural bond orbital (NBO) analysis, Industrial Thechnologies, 3 (2016) 151–154.

[13] Yankova, R., Structural and electronic properties of [Cd(benzimidazole)2Cl2], Science & Technologies, 6 (2016) 63–70.

[14] Bukowska-Strzyżewska, M., A. Tosik, Crystal and molecular structure of dibromobis (benzimidazole) copper (II), Journal of Chemical Crystallography, 18 (1988) 525–531.

[15] C.T. Lee, W.T. Yang, R.G. Parr, Development of the Colle-Salvetti correlation-energy formula into a functional of the electron density, Phys. Rev., B 37 (1988) 785–789.

[16] A.D. Becke, Densityfunctional thermochemi-stry. III. The role of exact exchange, J. Chem. Phys., 98 (1993) 5648–5652.

[17] R.G. Parr, W. Yang, Density-functional theory of atoms and molecules (Vol. 16), Oxford university press, 1989.

[18] R. Dennington, T. Keith, J. Millam, GaussView, Version 5, Semichem Inc., Shawnee Mission, KS, 2009.

[19] Hoffmann, R., A chemical and theoretical way to look at bonding on surfaces, Reviews of modern Physics 60 (1988) 601–628.

[20] M.J. Frisch, G.W.Trucks, H.B.Schlegel, G.E.Scuseria, M.A.Robb, J.R.Cheeseman, J.A.Montgomery Jr.,T.Vreven, K.N.Kudin, J.C.Burant, J.M.Mill¬am, S. S.Iyengar, J.Tomasi, V.Barone, B.Mennu¬cci, M.Cossi, G.Scalmani, N.Rega, G.A.Peter¬sson, H.Nakatsuji, M.Hada, M.Ehara, K.Toyota, R.Fukuda, J.Hasegawa, M.Ishida, T.Nakajima, Y.Honda, O.Kitao, H.Nakai, M.Klene, X.Li, J.E.Knox, H.P.Hratchian, J.B.Cross, V.Bakken, C.Adamo, J.Jaramillo, R.Gomperts, R.E.Strat¬mann, O.Yazyev, A.J.Austin, R.Cammi, C.Po¬me¬lli, J.W.Ochterski, P.Y.Ayala, K.Morokuma, G.A.Voth, P.Salvador, J.J.Dannenberg, V.G.Za¬krzewski, S.Dapprich, A.D.Daniels, M.C.Strain, O.Farkas, D.K.Malick, A.D.Rabuck, K.Rag¬havachari, J.B.Foresman, J.V.Ortiz, Q.Cui, A.G. Ba¬boul, S.Clifford, J.Cioslowski, B.B.Stefanov, G.Liu, A.Liashenko, P.Piskorz, I.Komaromi, R. L.¬Martin, D.J.Fox, T.Keith, M.A.Al-Laham, C. Y.Peng, A.Nanayakkara, M.Challacombe, P.M. W.Gill, B.Johnson, W.Chen, M.W.Wong, C. Gon¬za¬lez, J.A.Pople, Gaussian 03, Revision B.04, Gaussian, Inc., Wallingford CT, 2004.

[21] Gunasekaran, S., R.A. Balaji, S. Kumeresan, G. Anand, S. Srinivasan, Experimental and theoretical investigations of spectroscopic properties of N-acetyl-5-methoxytryptamine, Can. J. Anal. Sci. Spectrosc, 53 (2008) 149–160.

[22] Wolinski, K., J.F. Hinton, P. Pulay, Efficient implementation of the gauge-independent atomic orbital method for NMR chemical shift calculations, Journal of the American Chemical Society, 112 (1990) 8251–8260.

[23] Sastri V.S., J.R. Perumareddi, Molecular orbital theoretical studies of some organic corrosion inhibitors, Corros. Sci., 53 (1997) 617–622.

[24] Pearson, R.G., Hard and soft acids and bases, Journal of the American Chemical Society, 85 (1963) 3533–3539.

[25] Pearson, R.G., Absolute electronegativity and hardness correlated with molecular orbital theory, Proceedings of the National Academy of Sciences, 83 (1986) 8440–8441.

[26] Parr R.G., W. Yang, Density-Functional Theory of Atoms and Molecules, Oxford University Press, New York, 1989.

[27] Kavitha, E., N. Sundaraganesan, S. Sebastian, Molecular structure, vibrational spectroscopic and HOMO, LUMO studies of 4-nitroaniline by density functional method, Indian J. Pure Appl. Phys., 48 (2010) 20–30.

[28] Parr, R.G., V.S. Laszlo, L. Shubin, Electrophilicity index, Journal of the American Chemical Society, 121 (1999) 1922–1924.

[29] J.S. Murray, K. Sen, Molecular Electrostatic Potentials, Concepts and Applications, Elsevier, Amsterdam, 1996.

[30] E. Scrocco, J. Tomasi, in: P. Lowdin (Ed.), Advances in Quantum Chemistry, Academic Press, New York, 1978.

[31] M. Karabacak, M. Çınar, M. Kurt, An experimental and theoretical study of molecular structure and vibrational spectra of 2-chloronicotinic acid by density functional

theory and ab initio Hartree–Fock calculations, J. Molec. Str., 885 (2008) 28–35.

[32] W.R. Augus, C.K. Ingold, A.H. Leekie, J. Chem. Soc, (1936) 925.

[33] C.R. Bailey, S.C. Carson, R.R. Gordon, C.K. Ingold, Structure of benzene. Part XIX. The infrared spectra of 1:4-dideuterobenzene and 1:2:4:5-tetradeuteroben¬zene: description and analysis, Journal of the Chemical Society, 63 (1946) 288–299.

[34] E.F. Mooney, The infrared spectra of chlorobenzene and bromobenzene derivatives–III. Toluenes, Spectrochimica Acta 20.9 (1964)1343–1348.

[35] G. Joshi, N.L. Singh, Infrared absorption spectrum of orthofluorotoluene, Spectrochimica Acta Part A: Molecular Spectroscopy, 23.5 (1967) 1341–1344.

[36] M. Tsuboi, 15 N isotope effects on the vibrational frequencies of aniline and assignments of the frequencies of its nh 2 group, Spectrochimica Acta, 16.4 (1960) 505–512.

[37] C.S. Venkateswaran, N.S. Pandya, The Raman spectra of organic compounds: aniline. Proceedings of the Indian Academy of Sciences-Section A., Springer India, 15(5) (1942) 390–395.

[38] J.C. Evans, The vibrational assignments and configuration of aniline, aniline-NHD and aniline-ND 2, Spectrochimica Acta, 16.4 (1960) 428–442.

[39] S. Pinchas, David Samuel, Marta Weiss-Broday, The infrared absorption of 18 O-labelled benzamide, Journal of the Chemical Society, (1961) 1688–1692.

[40] L. Kahovec, K.F. Kohlrausch, Studien zum Raman-Effekt. Monatshefte für Chemie/Chemical Monthly, 74.1 (1941) 104–117.